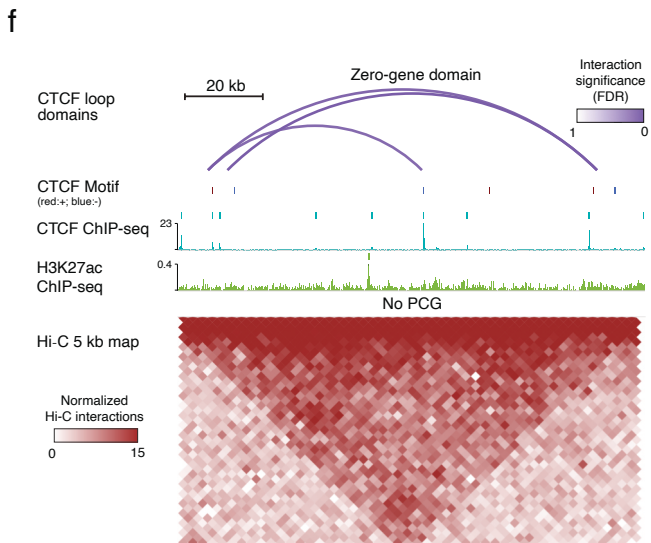
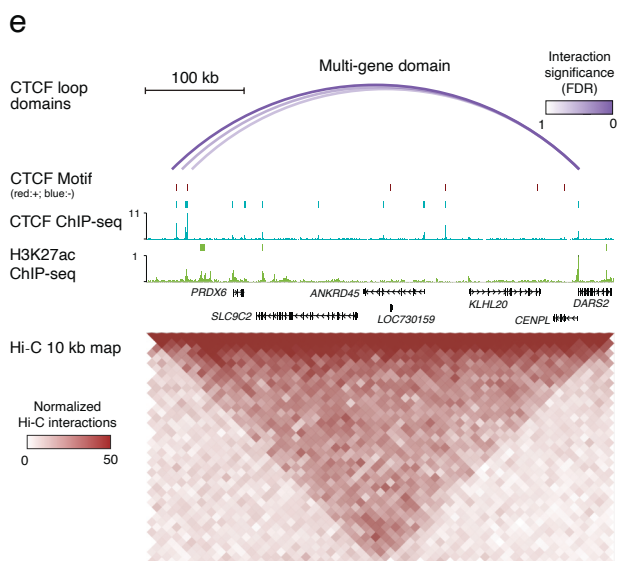
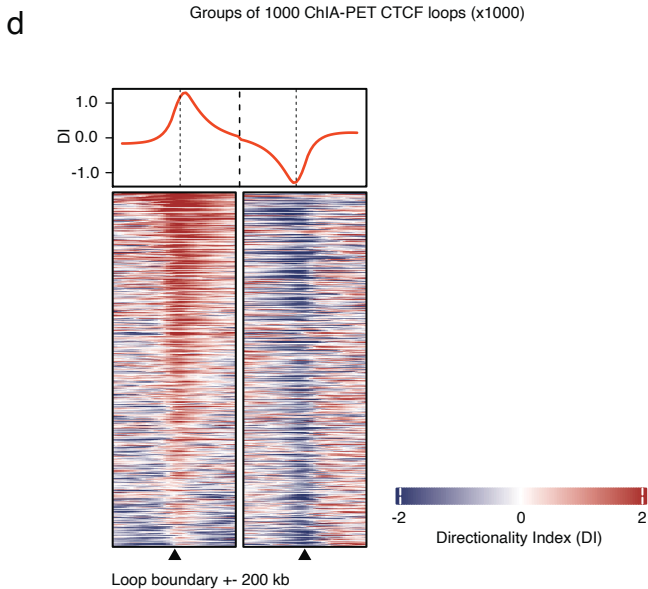
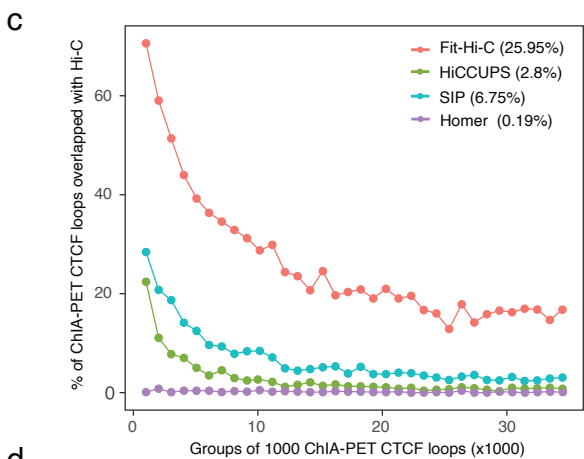
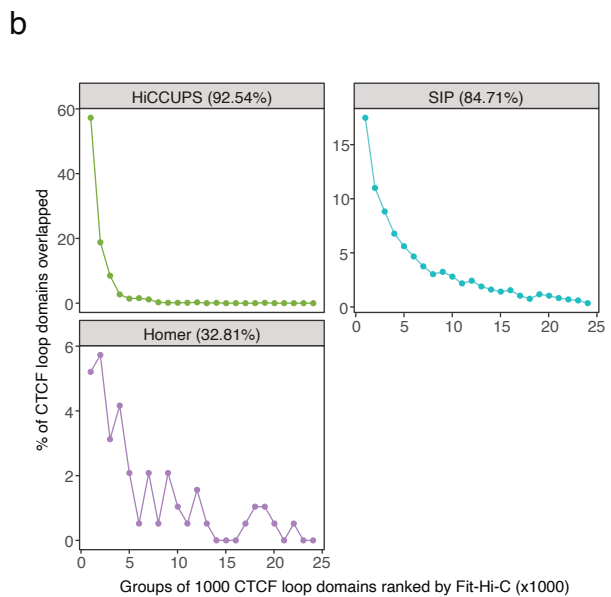
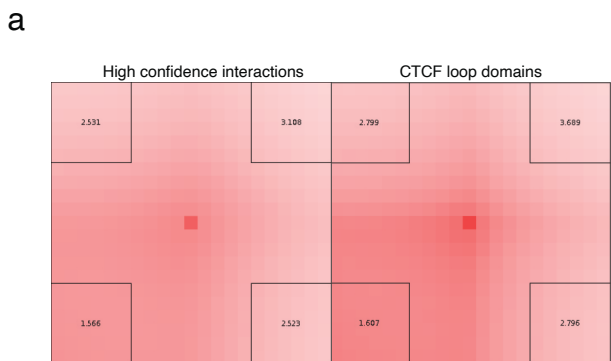


## **Topological isolation of developmental regulators in mammalian genomes**

Hua-Jun Wu, Alexandro Landshammer, Elena Stamenova, Adriano Bolondi, Helene Kretzmer, Alexander Meissner, and Franziska Michor





**Supplementary Fig. 1: Identification and classification of CTCF loop domains in HUES64 cell line.**

**(a)** Aggregate peak analysis (APA) plot for 231,970 high confidence interactions and 24,056 CTCF loop domains called from HUES64 Hi-C data. The APA score (number in the four corners outlined by the black box) is the ratio of the number of contacts in the central bin to the mean number of contacts in the corner.

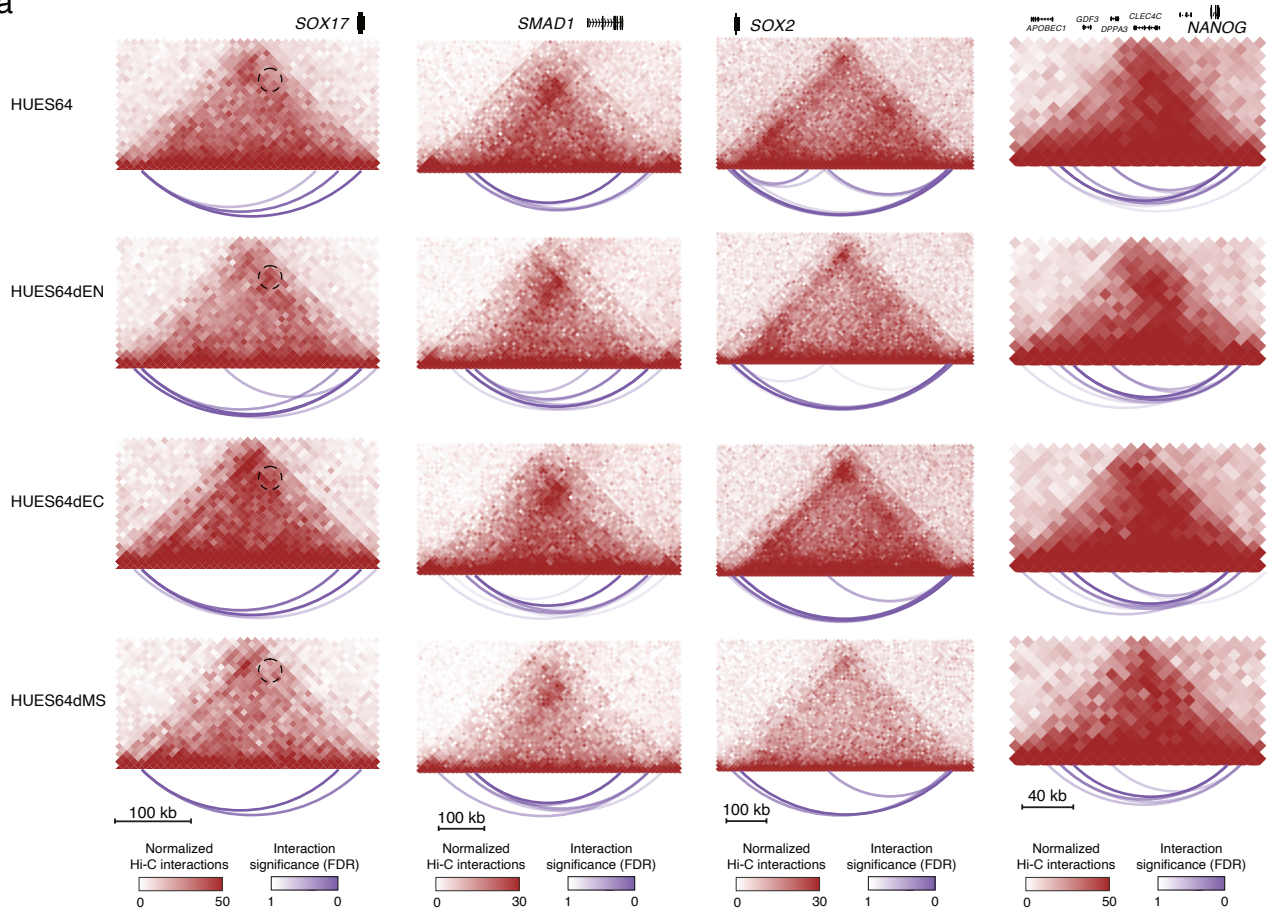
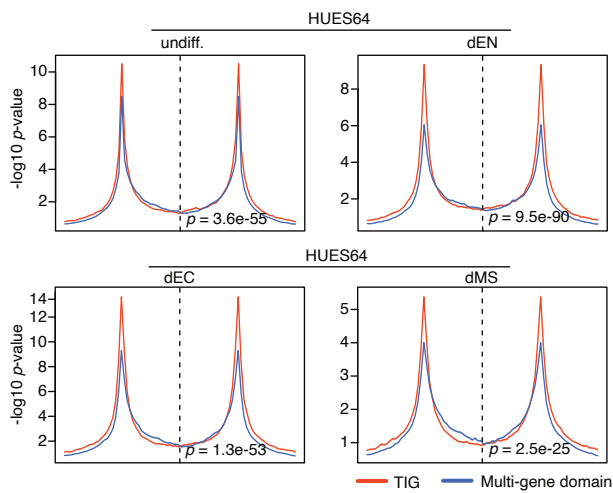
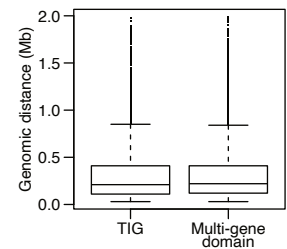
**(b)** Comparisons of CTCF loop domains identified by Fit-Hi-C and other methods. The percent of CTCF loop domains overlapping between Fit-Hi-C and HiCCUPS, SIP, Homer in HUES64 Hi-C data are plotted for loops ranked from the most significant to the least significant by Fit-Hi-C. Each point represents 1000 loops. The total percentage of CTCF loop domains overlapping for each method is shown in parentheses on top of each subplot. The CTCF loop domains are defined to be exactly the same without any shift in this analysis.

**(c)** The percent of insulated neighborhoods identified by ChIA-PET overlapping with CTCF loop domains obtained by different methods in Hi-C data are plotted for insulated neighborhoods ranked by ChIA-PET data from the most significant to the least significant. The total percentages of insulated neighborhoods overlapping with different Hi-C methods are shown in parentheses in the legend. Each point represents 1000 loops. Insulated neighborhoods in ChIA-PET were obtained from the supplementary table of the original paper.

**(d)** Directionality Indices (DI) obtained from 10 kb Hi-C map in HUES64 cells by Homer are plotted for the surrounding regions (200 kb upstream and downstream) of the left and right CTCF loop domain boundaries to depict their insulation function. The left heatmap shows the surrounding regions of the left boundary, and the right heatmap shows the surrounding regions of the right boundary. Each row represents one CTCF loop domain. Black arrow heads represent the left and right boundaries. The average profiles are shown on top of the heatmap. Higher signal in the left heatmap represents entering an insulated region, and lower signal in the right heatmap represents exiting an insulated region.

**(e)** Display of a multi-gene CTCF loop domain at *PRDX6* locus. Tracks are shown in the same way as in **Fig. 1c**, except each pixel in Hi-C plot represents 5-kb genomic region.

**(f)** Display of zero-gene CTCF loop domain at chr1:5680000-5920000. Tracks are shown in the same way as in **Fig. 1c**, except each pixel in Hi-C plot represents 5-kb genomic region.

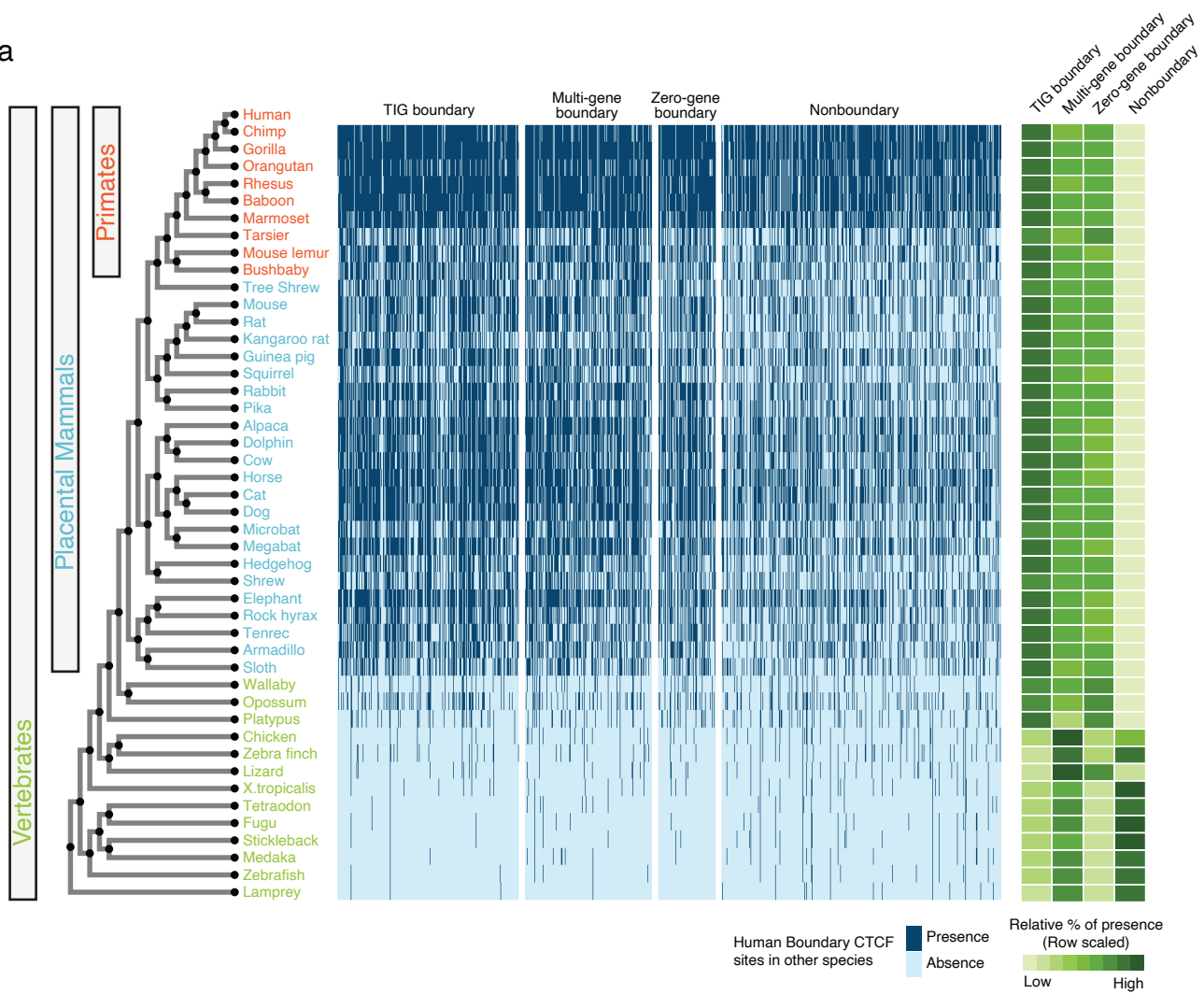
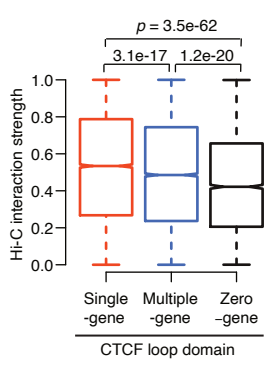
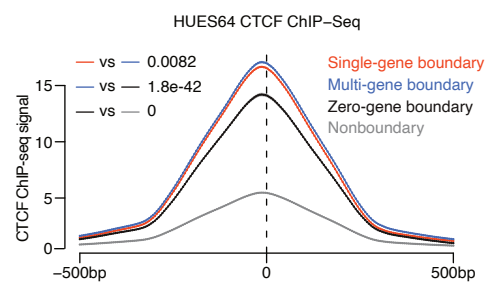
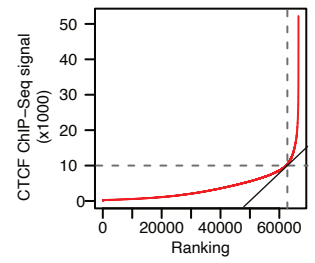
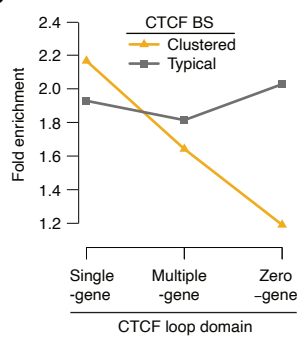
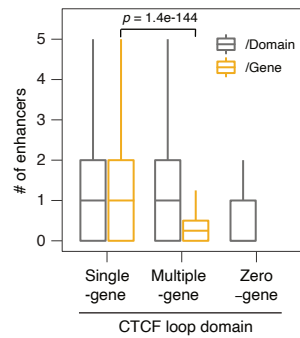
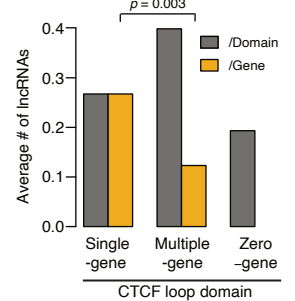
**a****b****c**

**Supplementary Fig. 2: Boundaries of CTCF loop domains.**

**(a)** Preserved pattern of CTCF loop domains during ES differentiation exemplified at *SOX17*, *SMAD1*, *SOX2* and *NANOG* loci. Normalized Hi-C interactions are shown as a heatmap with each pixel representing a 10-kb genomic region. The interaction significance (FDR) was calculated from Hi-C data, and is shown as arcs. Circles in the *SOX17* locus represent the interactions between *SOX17* promoter and distal enhancers induced in endoderm.

**(b)** Boundary-anchored virtual 4-C average profile of the CTCF loop domain boundaries in HUES64 and its derivatives. The locations of CTCF loop domain boundaries were identified in HUES64 Hi-C data. The  $-\log_{10}$  p-values obtained from Fit-Hi-C data are shown. The dotted line separates the left and right boundary regions, which represent the regions in the left and right heatmap in Fig. 2A. Average signals across all boundaries are shown with the shaded area indicating the standard error. Two-sided Wilcoxon test was used to determine the significance level of boundary-to-boundary interactions between the two groups. Data are presented as mean values  $\pm$  SE.

**(c)** The distribution of genomic distances spanning CTCF loop domains of TIGs and nonTIGs. The box indicates the interquartile range (IQR), the line inside the box shows the median, and whiskers show the locations of either  $1.5 \times$  IQR above the third quartile or  $1.5 \times$  IQR below the first quartile,  $n = 3310$  boundary-to-boundary interactions for TIG,  $n = 8729$  boundary-to-boundary interactions for multi-gene domain.

**a****b****c****d****e****f****g**

**Supplementary Fig. 3: Characterization of different types of CTCF loop domains.**

**(a)** Presence or absence of human CTCF motifs in 45 vertebrates. CTCF motifs were grouped based on the CTCF loop domain classification in HUES64 cell line. The relative proportion of present motifs in each group per species were calculated and shown in the right panel. Specifically, the absolute proportion of present motifs was calculated and row z-scored to obtain the relative proportion of present motifs. The phylogenetic tree is obtained from UCSC genome browser.

**(b)** The strength of Hi-C interactions in different types of domains. The significance ( $-\log_{10}$  p value) of Hi-C interaction is rank normalized and displayed in y-axis with “1” represents most significant interactions and “0” represents least significant interactions. The box indicates the interquartile range (IQR), the line inside the box shows the median, and whiskers show the locations of either  $1.5 \times$  IQR above the third quartile or  $1.5 \times$  IQR below the first quartile,  $n = 9673$  single-gene domains,  $n = 9189$  multiple-gene domains,  $n = 5194$  zero-gene domains. P values calculated by two-sided Wilcoxon test.

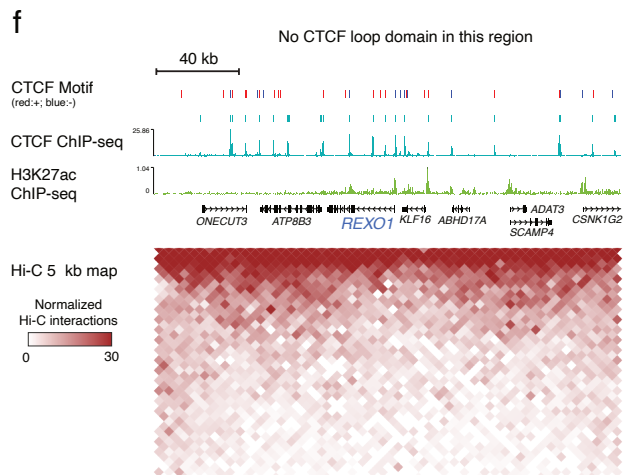
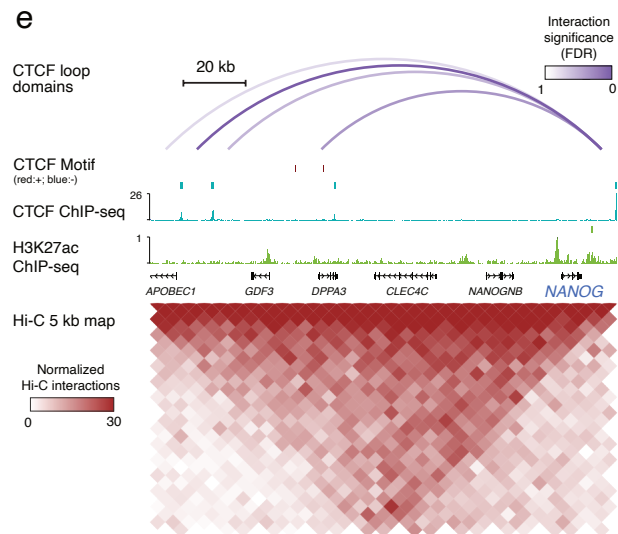
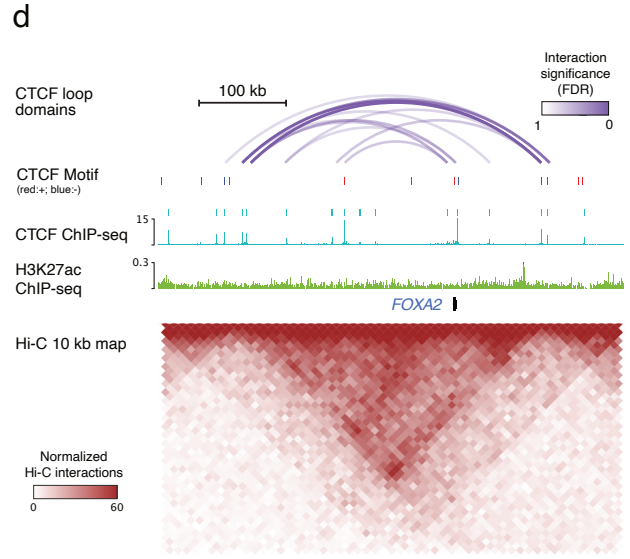
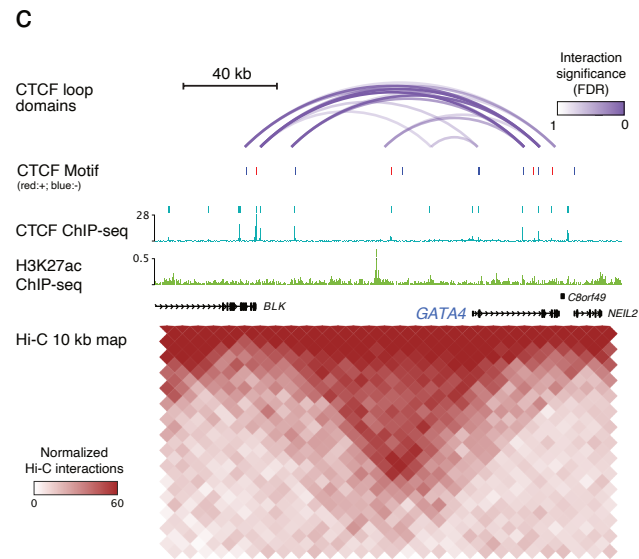
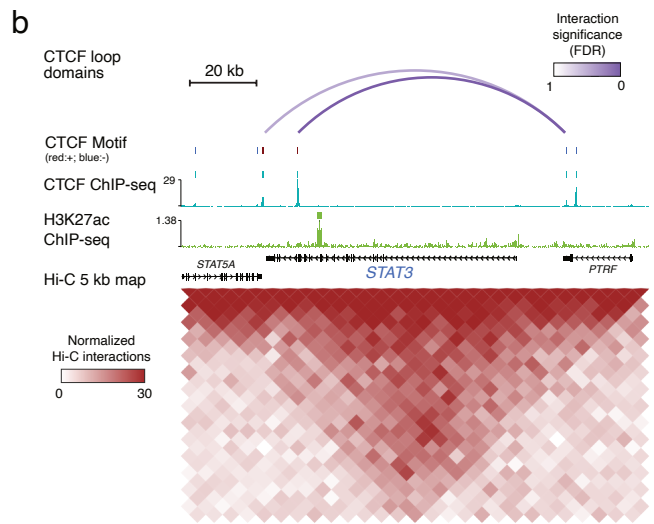
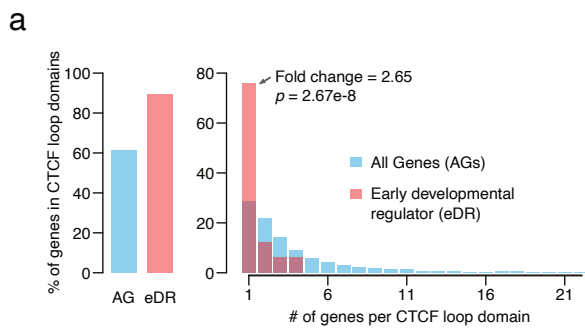
**(c)** CTCF ChIP-Seq signal of consensus CTCF motifs at boundaries of single-gene, multi-gene, and zero-gene CTCF loop domains and nonboundaries. See other descriptions in Fig. 3C.

**(d)** CTCF ChIP-seq signal of stitched peaks (y-axis) is plotted against the rank of the signal from low to high. Transition point was identified as described in Methods. Peaks above the point is clustered CTCF sites, while peaks below the point is typical CTCF sites.

**(e)** Fold enrichment of clustered and typical CTCF binding sites (CTCF BS) in the boundaries of different types of domains. Clustered CTCF binding sites have broader and more CTCF binding based on the ChIP-seq experiment.

**(f)** The number of enhancers per domain (or per gene) within different types of domains. Grey represents the number of features per domain, and orange represents the number of features per gene. The box indicates the interquartile range (IQR), the line inside the box shows the median, and whiskers show the locations of either  $1.5 \times$  IQR above the third quartile or  $1.5 \times$  IQR below the first quartile,  $n = 9673$  single-gene domains,  $n = 9189$  multiple-gene domains,  $n = 5194$  zero-gene domains. P values calculated by two-sided Wilcoxon test.

**(g)** The average number of long non-coding RNAs (lncRNAs) within different types of domains. P values calculated by two-sided Wilcoxon test.



**Supplementary Fig. 4: Early developmental regulators in CTCF loop domains.**

**(a)** Enrichment of early developmental regulators in single-gene domains. The left panel represents the percent of all genes (AG) or early developmental regulators (eDR) located within domains. The right panel represents the percent of AG or eDR located within domains with increasing number of protein coding genes. P-values calculated by two-sided Fisher's exact test.

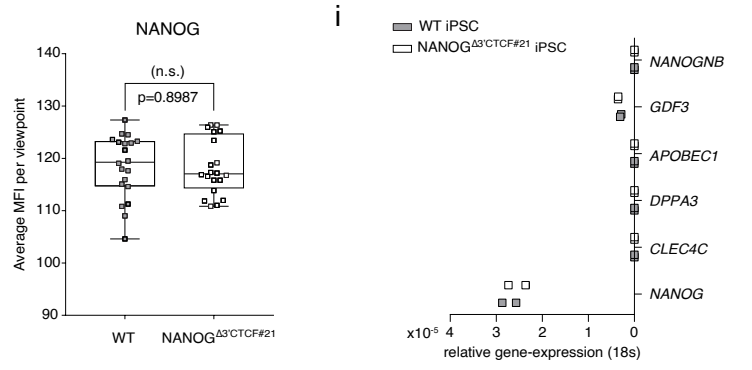
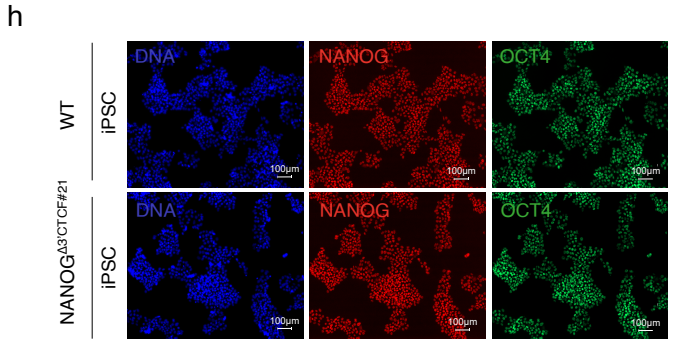
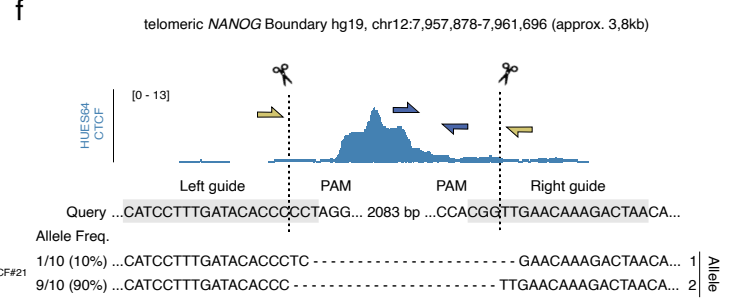
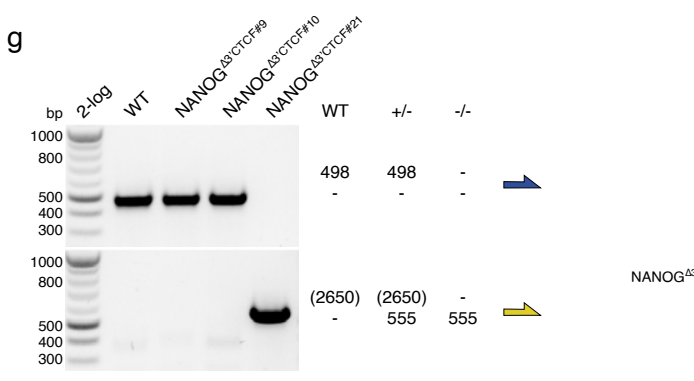
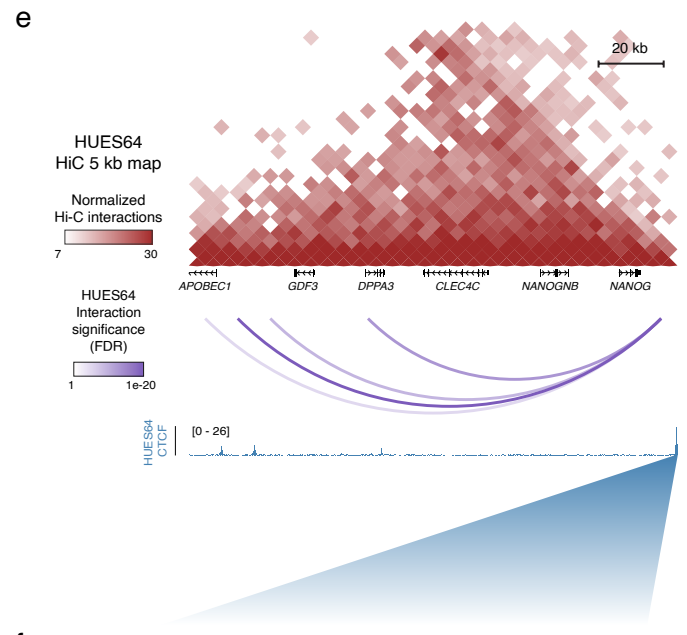
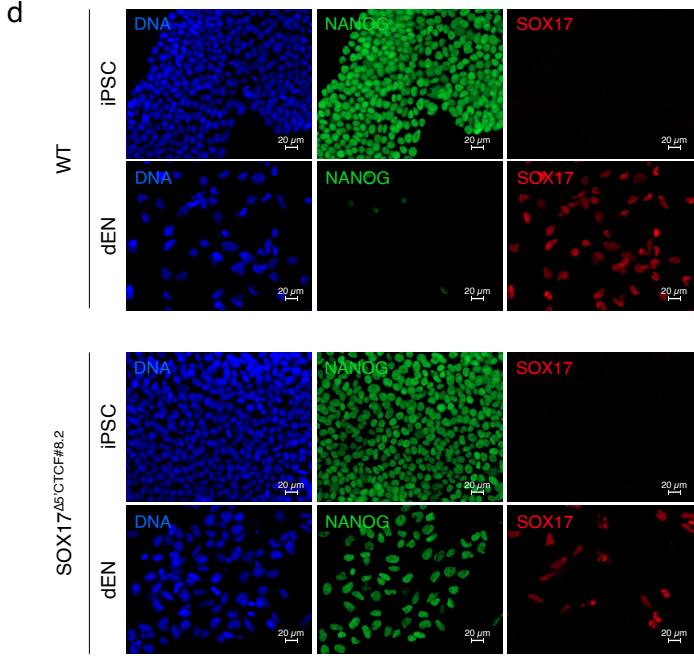
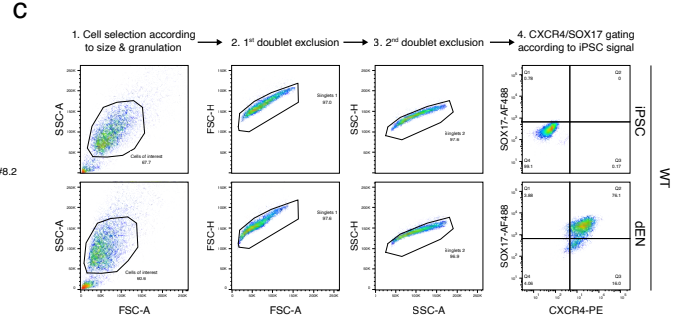
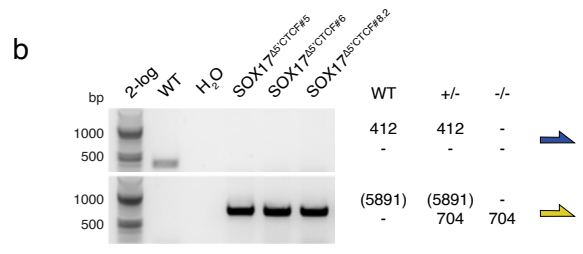
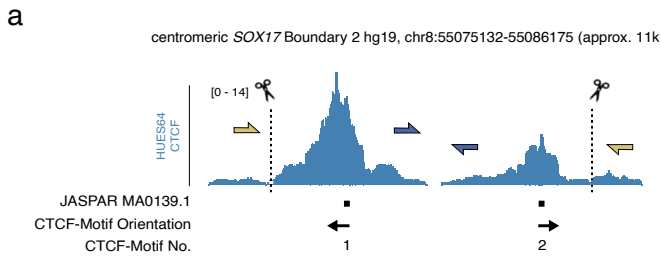
**(b)** Display of genomic locus at *STAT3* as a TIG that is in a single-gene domain. Domains displayed as arcs overlayed on top of CTCF and H3K27ac ChIP-seq profiles and normalized Hi-C interaction map. CTCF peaks and enhancers are denoted as bars above the ChIP-seq profiles of CTCF and H3K27ac. CTCF consensus motifs are denoted as red (forward orientation) and blue (reverse orientation) bars above the CTCF peaks. Normalized Hi-C interactions are denoted as heatmap with each pixel represents 5-kb genomic region. The interaction significance (FDR) was calculated from Hi-C data.

**(c)** Display of genomic locus at *GATA4* as a TIG that is in a single-gene domain. Tracks are shown in the same way as in **(a)**.

**(d)** Display of genomic locus at *FOXA2* as a TIG that is in a single-gene domain. Tracks are shown in the same way as in **(a)**.

**(e)** Display of genomic locus at *NANOG* that is in a multi-gene domain. Tracks are shown in the same way as in **(a)**.

**(f)** Display of genomic locus at *REXO1* that is not in a domain. Tracks are shown in the same way as in **(a)**.





**Supplementary Fig. 5: Phenotype of *SOX17* TIG boundary, and *NANOG* CTCF loop domain boundary perturbation.**

**(a)** Centromeric *SOX17* boundary ( $SOX17^{\Delta 5'CTCF}$ ) targeting strategy scheme. Scissors and dashed lines indicate CRISPR/Cas9 target-sites. Representative chromatogram-data including allele-frequency of sanger-sequenced, pJET1.2 cloned PCR-products of clone  $SOX17^{\Delta 5'CTCF\#8.2}$  are depicted below.

**(b)** Expected PCR-band pattern for different primer-pairs of centromeric *SOX17* boundary targeting are indicated by primer color. 1% agarose-gel pictures depict genotyping PCR band size-separations of respective knockout clone and control gDNA.

**(c)** FlowJo gating strategy example. Cells were selected according to size and granulation (1) followed by single cell selection (2-3). In case of *SOX17/CXCR4*, cell population percentages considered positive (4) are based on cell selections according to iPSC signal.

**(d)** Immunofluorescent stainings of *NANOG*, *SOX17* and DNA (DAPI) from day 0/5 *in vitro* endoderm differentiated  $SOX17^{\Delta 5'CTCF\#8.2}$  or wild type cells.

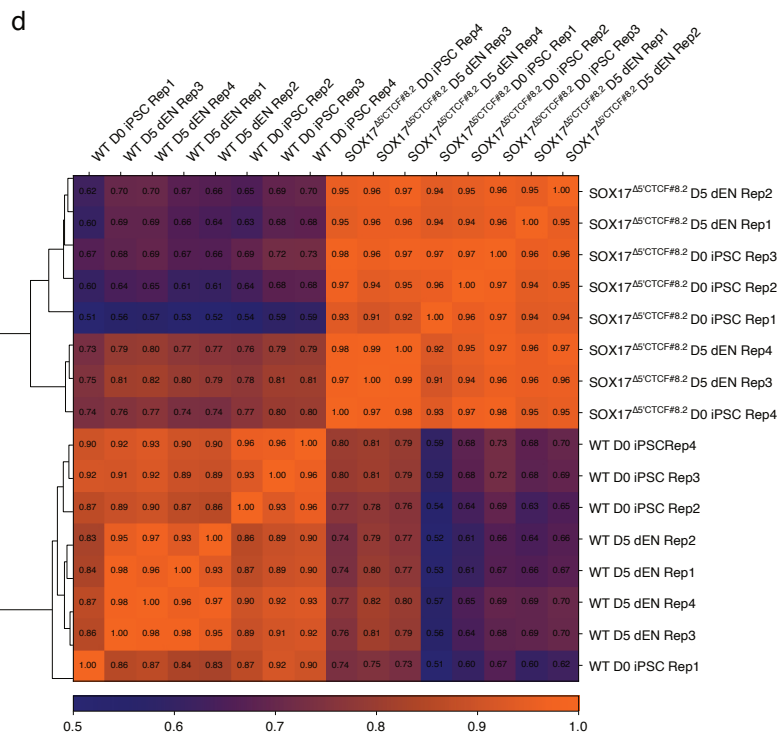
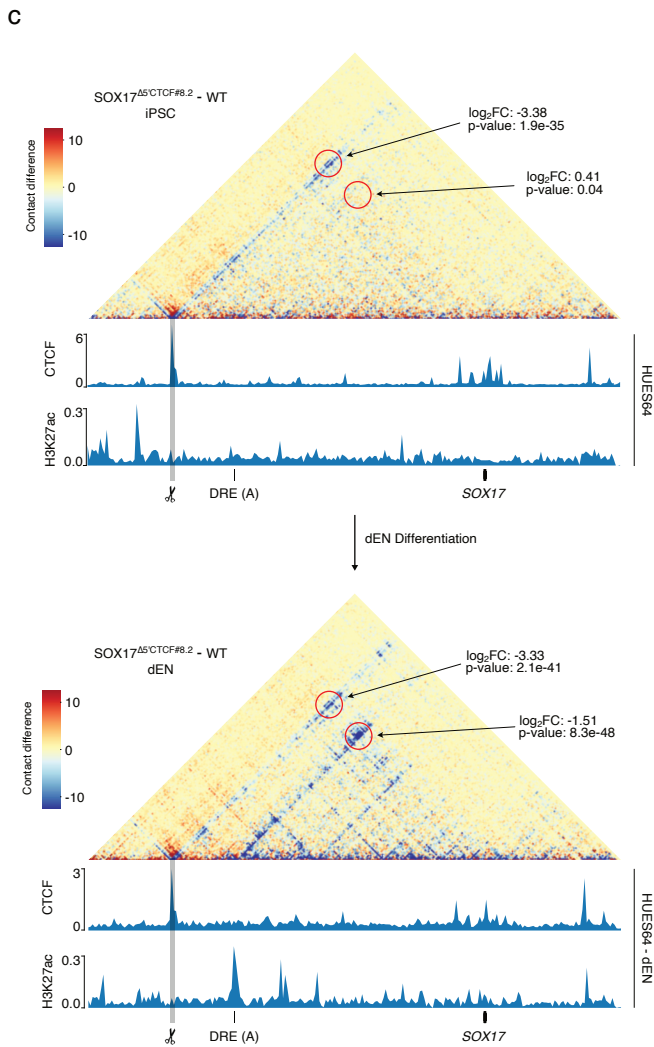
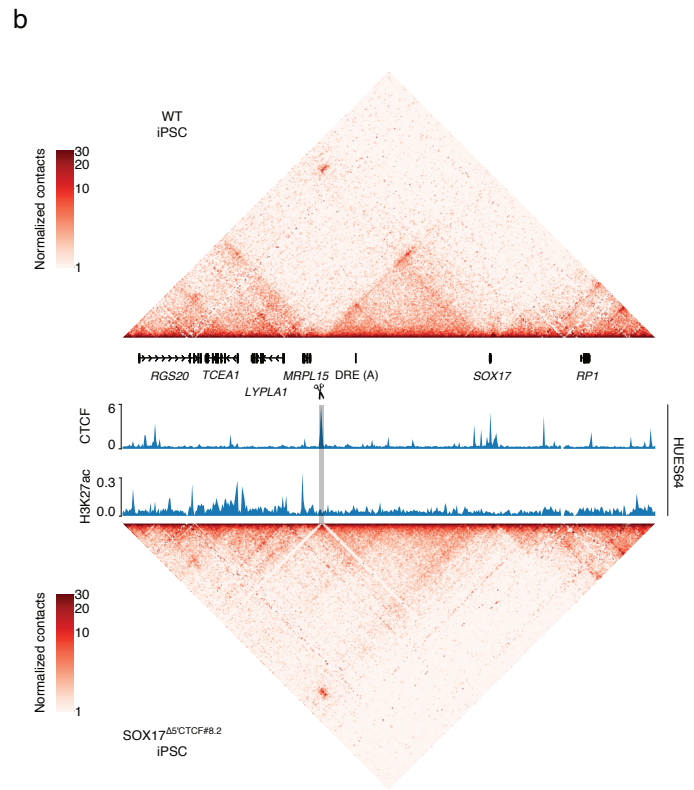
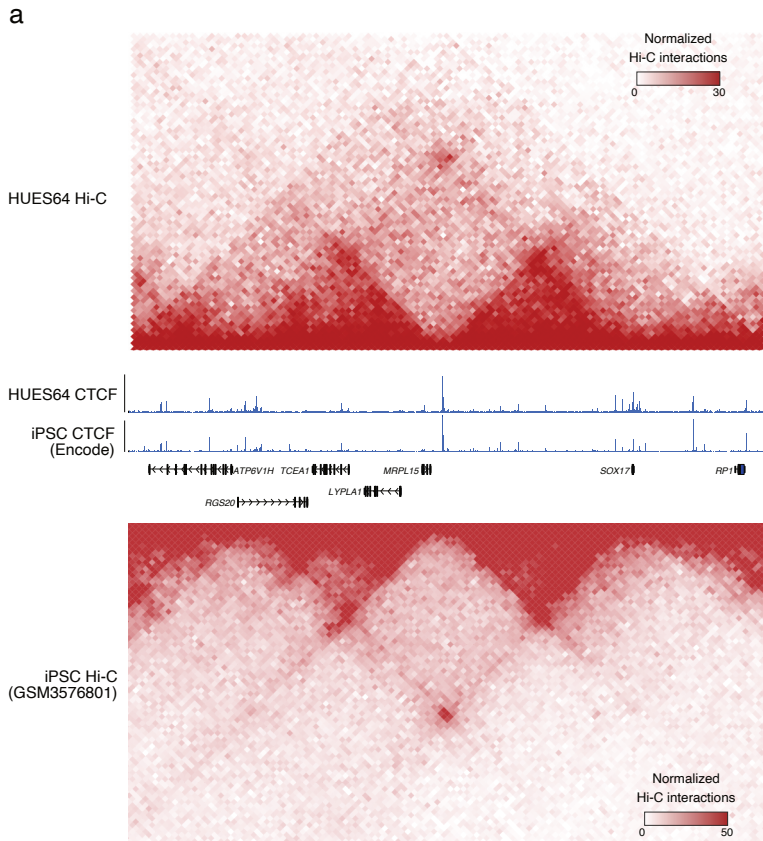
**(e)** Multi-layered display of the *NANOG* locus as a representative CTCF loop domain (multi-gene domain) at chr12: 7810000-7960000. HUES64 CTCF loop domains are displayed as arcs below a normalized Hi-C interaction map following by CTCF ChIP-seq profiles.

**(f)** Telomeric *NANOG* boundary ( $NANOG^{\Delta 3'CTCF}$ ) targeting strategy scheme. Targeting regions for the sgRNAs are depicted at the CTCF ChIP-seq profile indicated by dashed lines and scissors for the predicted Cas9 cut sites. Representative chromatogram-data including allele-frequency of sanger-sequenced, pJET1.2 cloned PCR-products of clone  $NANOG^{\Delta 3'CTCF\#21}$  are depicted below.

**(g)** Expected PCR-band pattern for different primer-pairs of telomeric *NANOG* boundary targeting are indicated by primer color. 1% agarose-gel pictures depict genotyping PCR band size-separations of respective knockout clone and control gDNA.

**(h)** Immunofluorescent stainings of *NANOG*, *OCT4* (*POU5F1*) and DNA (DAPI) from undifferentiated iPSC of  $NANOG^{\Delta 3'CTCF\#21}$  or wild type cells. Additionally, *NANOG* Mean fluorescence intensity (MFI) calculated in  $NANOG^{\Delta 3'CTCF\#21}$  and wild type iPSCs (n=10 independent regions (regional MFI average per cell) over 2 experiments with WT=20312 and  $NANOG^{\Delta 3'CTCF\#21}$ =17119 total cells). Statistical significance was determined by a two-tailed Mann Whitney U test. Data are presented as box plots, where the median is depicted as the box center, and 25% and 75% quartile are indicated as box bounds between whiskers that highlight minimum and maximum.

**(i)** qRT-PCR of bulk-populations from genes associated within the *NANOG* CTCF loop domain. Expression values are depicted as relative gene-expression ( $2^{-(\Delta Ct(GOI-18s))}$ ) (n=2 biological replicates).



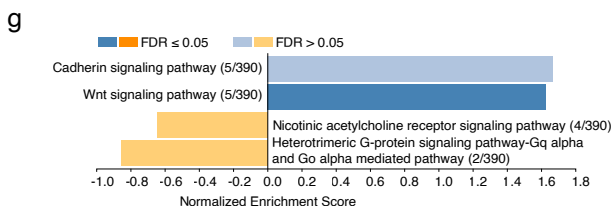
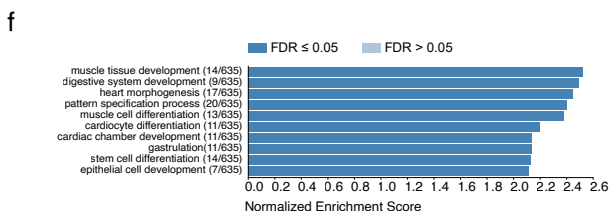
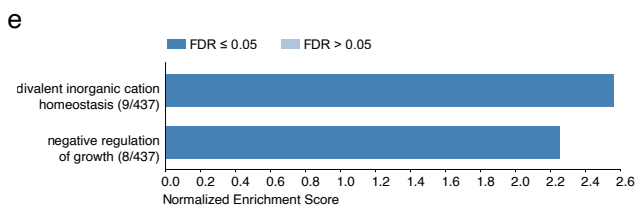
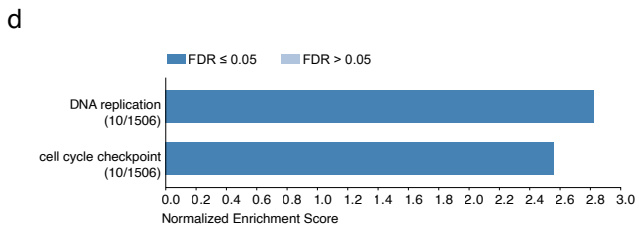
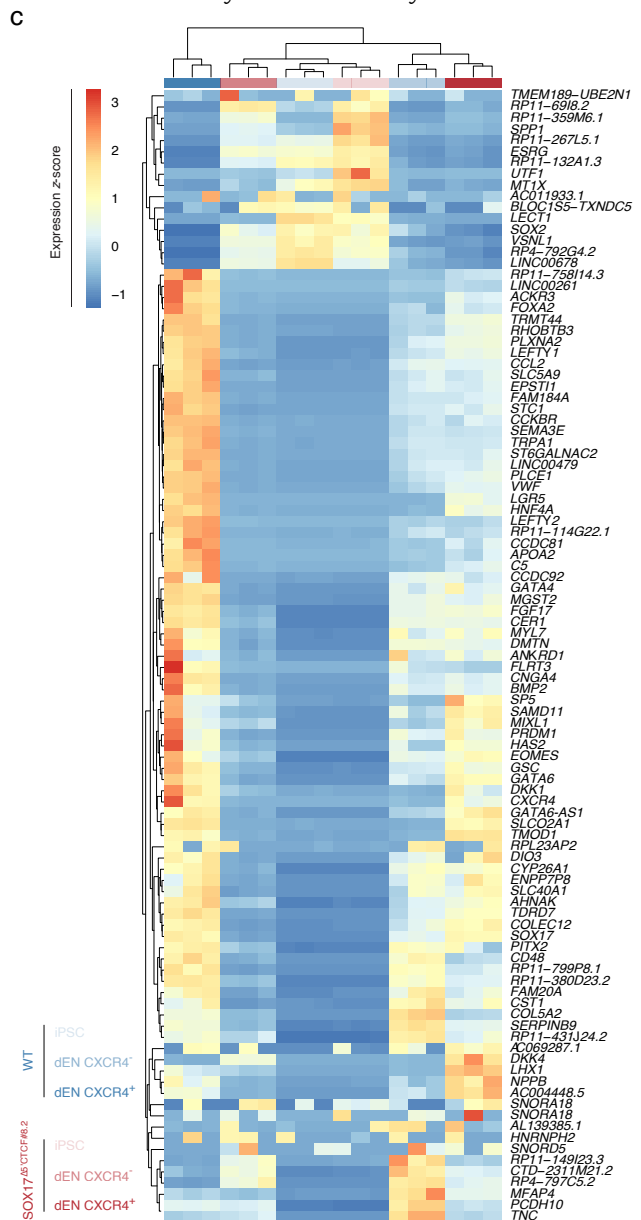
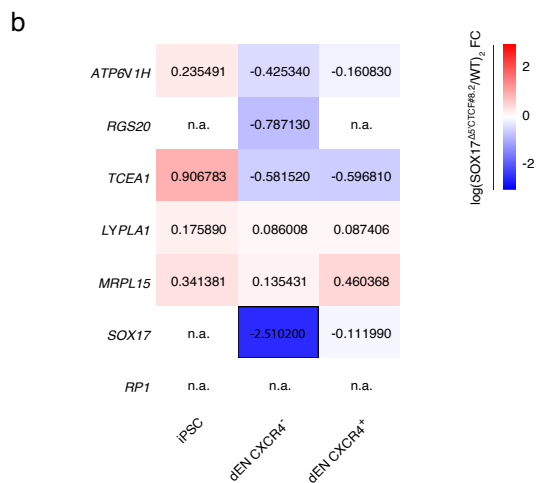
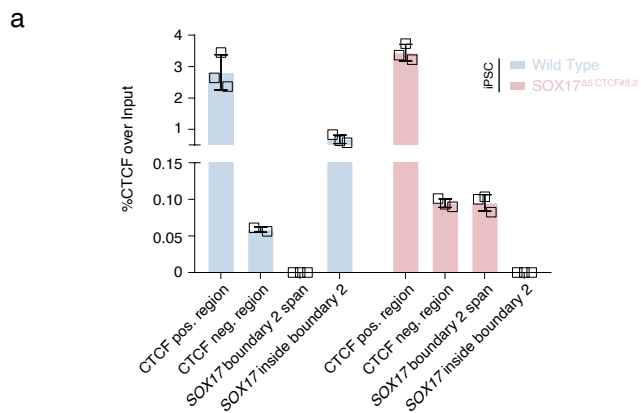
**Supplementary Fig. 6: cHi-C data analysis of *SOX17* TIG boundary perturbation.**

**(a)** Hi-C contact matrix and CTCF ChIP-seq of the *SOX17* locus in ES and iPSC cells. Hi-C matrix is provided in 10-kb resolution. CTCF iPSC is GM23338, and Hi-C iPSC is a mixture of reprogrammed cells from 7 individuals from iPSCORE.

**(b)** Capture Hi-C maps in iPSC wild type (upper panel) and *SOX17*<sup>Δ5'CTCF#8.2</sup> (lower panel) at the *SOX17* locus. The normalized capture Hi-C contact maps are overlaid with HUES64 CTCF and H3K27ac ChIP-seq profiles. The deleted centromeric *SOX17* boundary (Boundary 2) is highlighted in grey and marked by a scissor. Putative *SOX17* distal regulatory element DRE (A) and *SOX17* gene body are shown as black bars.

**(c)** Capture Hi-C subtraction maps in iPSC (upper panel) and dEN (lower panel) at the *SOX17* loop domain. The relative contact difference between the two samples (*SOX17*<sup>Δ5'CTCF#8.2</sup> – wild type) in either iPSC or dEN cells are shown on top of HUES64 or HUES64 derived dEN CTCF and H3K27ac ChIP-seq profiles. Boundary 1+2 contact quantifications and contact quantifications between DRE (A) and *SOX17* promoter are highlighted in red circles. The deleted centromeric *SOX17* boundary (Boundary 2) is highlighted in grey marked by a scissor. *SOX17* distal regulatory element DRE (A) and *SOX17* gene body is highlighted in black bars.

**(d)** Pair-wised pearson correlation between replicates of capture Hi-C data.



**Supplementary Fig. 7: CTCF ChIP-qRT-PCR, GSEA and gene-expression analysis of *SOX17* TIG boundary perturbation.**

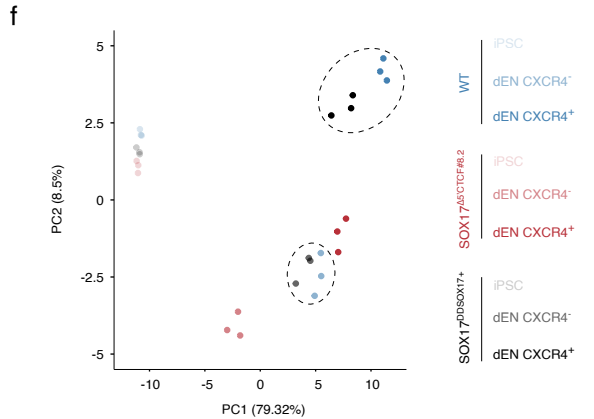
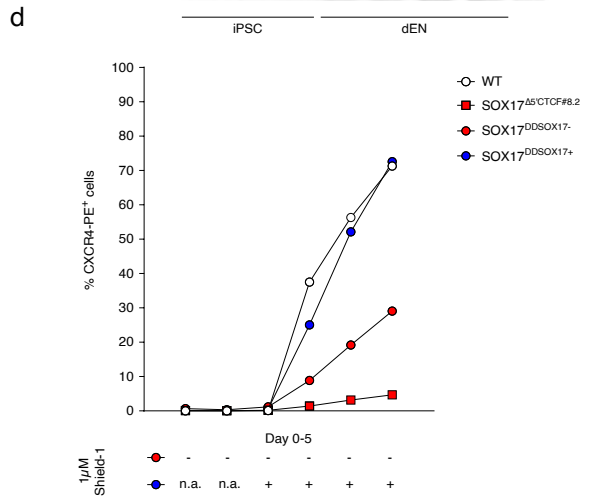
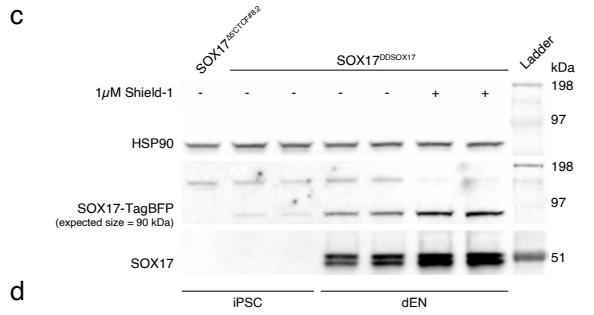
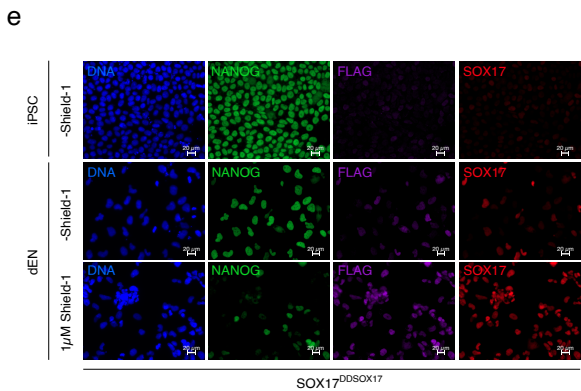
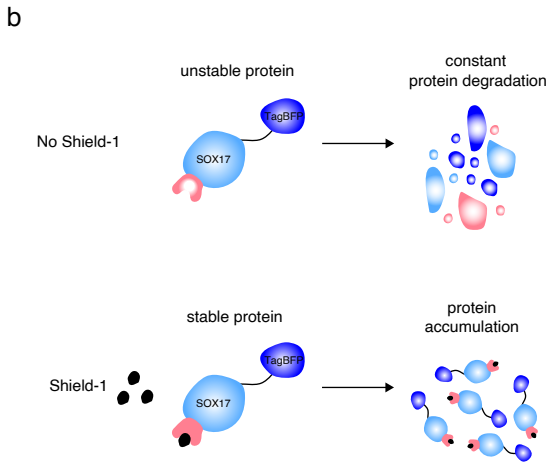
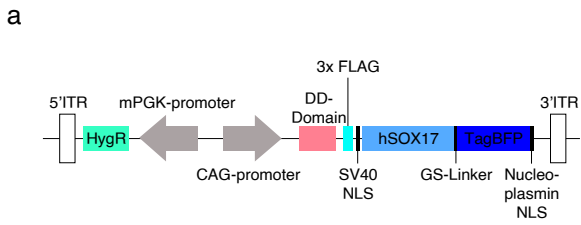
**(a)** CTCF ChIP-qRT-PCR of *SOX17* boundary 2 and control regions in undifferentiated *SOX17 $\Delta$ <sup>5'</sup>CTCF#8.2* or wild type iPSC. CTCF-enrichment is expressed as percentage of CTCF over input, at the respective site of interest (n=3 biological replicates). Data are presented as mean values +/- SD.

**(b)** TPM expression heatmap of genes associated with the *SOX17* locus. Expression values in iPSC, and *CXCR4*<sup>+/-</sup> dEN populations are depicted as  $\log(\text{SOX17}^{\Delta 5' \text{CTCF} \# 8.2} / \text{WT})_2 \text{FC}$ .

**(c)** TPM Z-score raw normalized clustering of the PCA-derived most variable genes (100) across different sub-populations.

**(d-f)** GO-terms of GSEA for biological processes from different sub-populations. FDRs are depicted by color.

**(g)** P-terms of GSEA for pathways (PANTHER) from different sub-populations. FDRs are depicted by color.



**Supplementary Fig. 8: SOX17 boundary rescue experiments by ectopic SOX17**

(a) Simplified 2D-model of the ITR-flanked piggy-BAC plasmid consisting of constitutively expressed Hygromycin selection marker sequence and inverse directed ectopic SOX17-TagBFP sequence flanked by nuclear localization signal sequence fused to the FKPB12 (L106P mut.) destabilizing domain sequence (DD-Domain).

(b) Schematic of default ectopic SOX17-TagBFP protein degradation and ProteoTuner™ system reversal of protein degradation in presence of Shield-1 compound.

(c) Western Blot data of day 0/5 *in vitro* endoderm differentiated SOX17<sup>DDSOX17-</sup> (-Shield1) or SOX17<sup>DDSOX17+</sup> (1μM Shield-1) cell lysates in comparison to SOX17<sup>Δ5<sup>'</sup>CTCF#8.2</sup> iPSC for SOX17 and HSP90 protein.

(d) Fluorescence activated cell sorting (FACS) time-course data of wild type, SOX17<sup>Δ5<sup>'</sup>CTCF</sup> and SOX17<sup>DDSOX17-/+</sup> iPSC during directed differentiation towards dEN. CXCR4 is depicted as percentage CXCR4<sup>+</sup> in bulk cell populations. Shield-1 ministered treatment schedule for SOX17<sup>DDSOX17+</sup> is shown below (n=2 biological replicates). Data are presented as mean values.

(e) Immunofluorescent stainings of NANOG, FLAG, SOX17 and DNA (DAPI) from day 0/5 *in vitro* dEN differentiated SOX17<sup>DDSOX17-</sup> (-Shield1) or SOX17<sup>DDSOX17+</sup> (1μM Shield-1) cells.

(f) Principal component analysis of RNA-seq data, depicting sample clusters by the use of the 100 most variable genes. The first two principal components (PCs) are displayed. Dashed lines indicate similarity between SOX17<sup>DDSOX17+</sup> rescued and wild type dEN cell CXCR4 sub-populations.





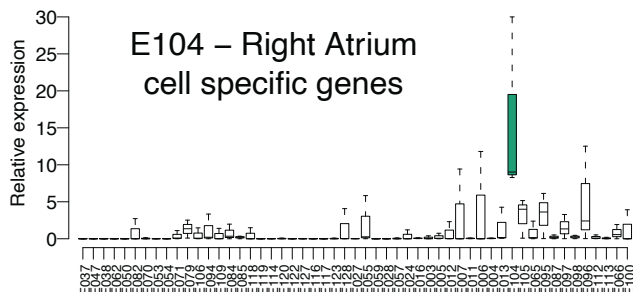
**Supplementary Fig. 9: Constitutive CTCF loop domains and their functions.**

**(a)** Examples of constitutive domains at the *SMAD2*, *GATA4*, *STAT3*, *LEF1*, *FOXA2* and *KLF5* loci that are conserved across 11-14 out of 16 human cell types. Arcs represent the consensus domains in different cell types with the darker color representing boundary interactions in more cell types. The most recurrent boundary interaction per locus is highlighted using a border line.

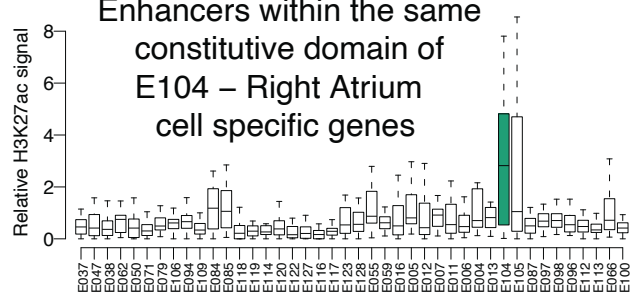
**(b)** Heatmap represents the expression profile of constitutive TIGs that overlap with cell type-specific regulators. Each row represents one gene. The gene names of each group are indicated by a word cloud, in which the frequencies of genes in the different samples of the same group are indicated. Larger font size represents higher frequency thus means the genes are highly expressed in more samples of the same group. Some regulators were recurrent across multiple cell lines of one type, such as *RUNX3* in immune cells, *RORB* in brain tissue, *ATOH1* in digestive tissue and *BNC1* in epithelial cells, while others were specific to one cell type, such as *SOX17* in endoderm and *MYB* in CD34<sup>+</sup> cells.

**a**

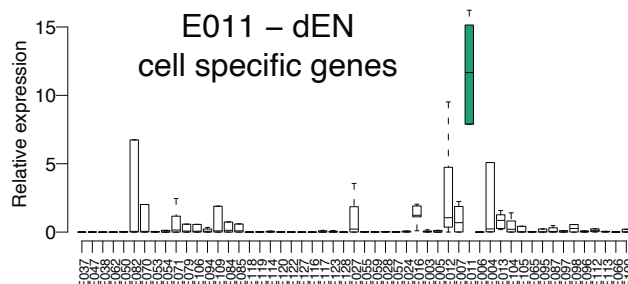
### E104 – Right Atrium cell specific genes



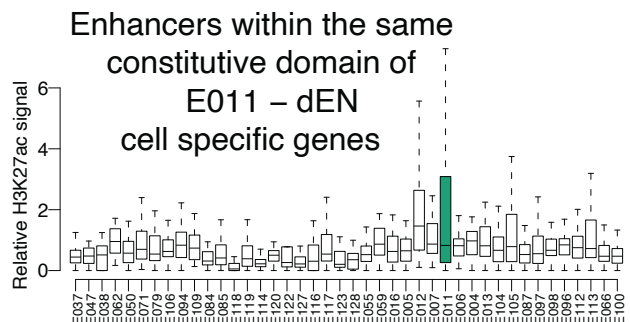
### Enhancers within the same constitutive domain of E104 – Right Atrium cell specific genes

**b**

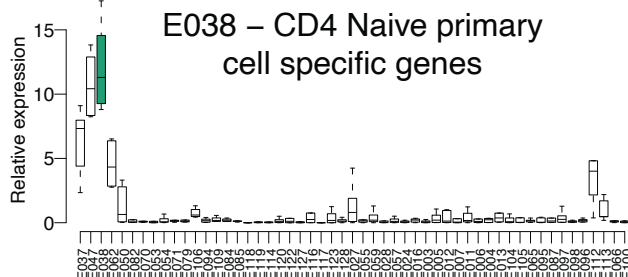
### E011 – dEN cell specific genes



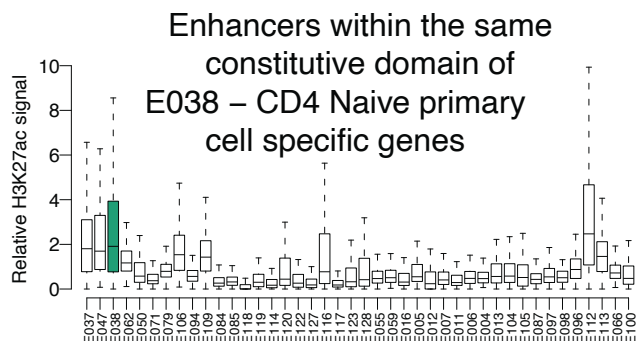
### Enhancers within the same constitutive domain of E011 – dEN cell specific genes

**c**

### E038 – CD4 Naive primary cell specific genes



### Enhancers within the same constitutive domain of E038 – CD4 Naive primary cell specific genes



**Supplementary Fig. 10: Co-activation patterns between cell type-specific regulators and enhancers insulated by constitutive CTCF loop domains.**

**(a)-(c) left panel**, Relative expression of cell type-specific regulators in E104, E011 and E038 across all cell types. Relative expression is the expression over mean expression across all cell types. The box indicates the interquartile range (IQR), the line inside the box shows the median, and whiskers show the locations of either  $1.5 \times \text{IQR}$  above the third quartile or  $1.5 \times \text{IQR}$  below the first quartile,  $n = 3$  genes for E104 (a),  $n = 6$  genes for E011 (b),  $n = 6$  genes for E038 (c).

**(a)-(c) right panel**, Relative H3K27ac abundance of enhancers located within the same constitutive domain of the cell type-specific regulators in E104, E011 and E038 across all cell types. Relative H3K27ac abundance is the H3K27ac signal over mean H3K27ac signal across all cell types that represents the enhancer activity. The box indicates the interquartile range (IQR), the line inside the box shows the median, and whiskers show the locations of either  $1.5 \times \text{IQR}$  above the third quartile or  $1.5 \times \text{IQR}$  below the first quartile,  $n = 27$  enhancers for E104 (a),  $n = 38$  enhancers for E011 (b),  $n = 166$  enhancers for E038 (c).



**Supplementary Fig. 11: Fold enrichment of cell type-specific regulators against the recurrence of TIGs in multiple cell types.** Each point represents 300 genes. Analysis in Fig. 7a is repeated for different threshold settings for identifying cell type-specific regulators. The results are consistent by changing the entropy setting from 0.7-0.9, and by changing the fold change settings from 5-10. Here fold change represents the case in which a gene has at least x-fold higher expression than the average expression of the gene in all cell types.

Supplementary Table 1. sgRNA sequences for boundary knock-out constructs.

Oligonucleotide Name	Purpose	5'-3' Sequence
SapI_sgRNA_casete_gBlock_+KpnI-sites	Extension cloning of PX458	tgcagacaaatggctctagaggtacggtaccAATATGCATT TTCCCATGATTCCCTTCATATTTGCATATAC GATACAAGGCTGTTAGAGAGATAAATTGGA ATTAATTTGACTGTAAACACAAAGATATT AGTACAAAATACGTGACGTAGAAAGTAAT AATTTCTTGGGTAGTTTGCAGTTTTAAAT TATGTTTTAAATGGACTATCATATGCTTA CCGTAACCTGAAAGTATTTTCGATTTCTTGG CTTTATATATCTTGTGGAAAGGACGAAAC ACCGGAAGAGCGAGCTCTTCTGTTTTAGA GCTAGAAATAGCAAGTTAAAATAAGGCTA GTCCGTTATCAACTTGAAAAAGTGGCACC GAGTCGGTGCTTTTTTGTTCCTGCAGGA GATTTagcgcgtgcgccaattctgcagacaaatggctctagagg taccggttacataacttacggtaatggA
AL_SOX17_CTCF_left_gRNA_1	CRISPR/Cas9 Targeting	TGTGGAAAGGACGAAACACCCATCCAGT CTGCCAACATAGTTTTAGAGCTAGAAATA GC
AL_SOX17_CTCF_left_gRNA_2	CRISPR/Cas9 targeting	TGTGGAAAGGACGAAACACCGGGCTGCAC CAAATCGCCACGTTTTAGAGCTAGAAATA GC
NANOG_CTCF_right_gRNA_1	CRISPR/Cas9 targeting	TGTGGAAAGGACGAAACACCCATCCTTTG ATACACCCCCTGTTTTAGAGCTAGAAATA GC
NANOG_CTCF_right_gRNA_2	CRISPR/Cas9 targeting	TGTGGAAAGGACGAAACACCTGTTAGTCT TTGTTCAACCGTTTTAGAGCTAGAAATAG C

Supplementary Table 2. Oligonucleotides used for genotype verification.

<b>Oligonucleotide Name</b>	<b>Purpose</b>	<b>hg19 Coordinates</b>	<b>5'-3' Sequence</b>
NANOG_spanbound_fwd	Genotyping	chr12:795813 2-7958151	GCCAGGGAGATAGGTGTGAA
NANOG_spanbound_rev	Genotyping	chr12:796076 2-7960781	GACTAGCTCACGTCATCCCC
NANOG_int_fwd	Genotyping	chr12:795925 7-7959278	GGTTGTGATCCCATTCATGTCA
NANOG_int_rev	Genotyping	chr12:795972 6-7959745	TCCCTTGTCCTGAACATGT
SOX17_spanbound_fwd	Genotyping	chr8:5507736 9-55077388	GCTCTGCACGTGGTAAAAGA
SOX17_spanbound_rev	Genotyping	chr8:5508324 0-55083259	TGAAGAGGACCATGAGCACA
SOX17_int_fwd	Genotyping	chr8:5507998 2-55080001	ACACGCTAAGCCACAATGAG
SOX17_int_rev	Genotyping	chr8:5508037 4-55080393	TTCTTCACAACCTTGCCAGC
pJet1.2_fwd	Genotyping	n.a.	CGACTCACTATAGGGAGAGCGGC
pJet1.2_rev	Genotyping	n.a.	AAGAACATCGATTTTCCATGGCAG

Supplementary Table 3. Antibodies used for FACS.

<b>Antibody name</b>	<b>Application / Dilution used</b>	<b>Clone / Company</b>	<b>Catalogue number</b>
Mouse anti-Human CRCX4 (CD184) PE	FACS / 1:200	12G5 / Biolegend	306506
Mouse IgG2 $\alpha$ PE Isotype control	FACS / 1:200	MOPC-173 / Biolegend	400212
Mouse anti-Human Ep-CAM (CD326) PE	FACS / 1:200	9C4 / Biolegend	324206
Mouse IgG2 $\beta$ PE Isotype control	FACS / 1:200	MPC-11 / Biolegend	400314
Mouse IgG1 $\kappa$ AlexaFluor488 Isotype control	FACS / 1:50	MOPC-21 / BD	557702
Mouse AlexaFluor488 SOX17	FACS / 1:50	P7-969 / BD	562205
Mouse AlexaFluor488 NANOG	FACS / 1:50	N31-355 / BD	560791



Supplementary Table 4. Antibodies used for Immunofluorescence staining and Western Blot.

<b>Antibody name</b>	<b>Application / Dilution used</b>	<b>Clone / Company</b>	<b>Catalogue number</b>
Rabbit anti-Human NANOG (unconjugated)	1 <sup>st</sup> IF / 1:1000	EPR2027(2) / Abcam	ab109250
Goat anti-Human SOX17 (unconjugated)	1 <sup>st</sup> IF & WB / 1:1000	Polyclonal / R&D Systems	AF1924
Mouse anti-Human OCT4 (unconjugated)	1 <sup>st</sup> IF / 1:2000	Polyclonal / Abcam	ab19857
Mouse anti-FLAG® M2 (unconjugated)	1 <sup>st</sup> IF / 1:1000	M2 / Sigma	F1804-50UG
Donkey anti-Mouse IgG AlexaFluor488	2 <sup>nd</sup> IF / 1:700	Polyclonal / Thermo Fisher Scientific	A21202
Donkey anti-Goat IgG AlexaFluor594	2 <sup>nd</sup> IF / 1:700	Polyclonal / Thermo Fisher Scientific	A11058
Donkey anti-Rabbit IgG AlexaFluor647	2 <sup>nd</sup> IF / 1:700	Polyclonal / Thermo Fisher Scientific	A31573

Supplementary Table 5. Antibodies only used for Western Blot.

<b>Antibody name</b>	<b>Application</b>	<b>Clone / Company</b>	<b>Catalogue number</b>
Mouse anti-Human HSP90 (unconjugated)	1 <sup>st</sup> WB / 1:4000	68/Hsp90 / BD	610419
Donkey anti-Mouse IgG HRP	1 <sup>st</sup> WB / 1:5000	Polyclonal / Jackson ImmunoResearch	715-035-150
Donkey anti-Goat IgG HRP	1 <sup>st</sup> WB / 1:5000	Polyclonal / Jackson ImmunoResearch	705-035-147

Supplementary Table 6. Oligonucleotide sequences used for CTCF ChIP qRT-PCR.

<b>Oligonucleotide Name</b>	<b>Purpose/Region</b>	<b>hg19 Coordinates</b>	<b>5'-3' Sequence</b>
CTCF_ChIPqPCR R_spanbound_fwd	ChIP qRT-PCR /KO span-region	chr8:5507772 9-55077748	GTGCCCTCCCCAAAACATTT
CTCF_ChIPqPCR R_spanbound_rev	ChIP qRT-PCR /KO span-region	chr8:5508313 9-55083158	GCCTGCTCTCAAAACCTTCA
CTCF_ChIPqPCR R_int_fwd	ChIP qRT-PCR /CTCF-motif 2	chr8:5508203 9-55082059	TGCAGTACCACATCTTGAACA
CTCF_ChIPqPCR R_int_rev	ChIP qRT-PCR /CTCF-motif 2	chr8:5508211 4-55082133	GCAAAACAACCTTACAGCGGC
CTCF_ChIPqPCR R_neg_fwd	ChIP qRT-PCR /neg. ctrl. region	chr8:5526255 4-55262573	TTGAGTCCCAGAGGTTGAGG
CTCF_ChIPqPCR R_neg_rev	ChIP qRT-PCR / neg. ctrl. region	chr8:5526260 9-55262628	GTCTCACTTTGTCCCCTGGG
CTCF_ChIPqPCR R_pos_fwd	ChIP qRT-PCR / pos. ctrl. region	chr8:5546441 8-55464437	GCCTTCAAAGCGGGTCATTT
CTCF_ChIPqPCR R_pos_rev	ChIP qRT-PCR / pos. ctrl. region	chr8:5546447 7-55464496	AACCCTCACAAACCCAGACA